

Optical properties of heavily boron-doped nanocrystalline diamond films studied by spectroscopic ellipsometry

A. Zimmer, O. A. Williams, K. Haenen, and H. Terryn

Citation: *Appl. Phys. Lett.* **93**, 131910 (2008); doi: 10.1063/1.2990679

View online: <http://dx.doi.org/10.1063/1.2990679>

View Table of Contents: <http://apl.aip.org/resource/1/APPLAB/v93/i13>

Published by the [American Institute of Physics](#).

Related Articles

Photoluminescence and secondary ion mass spectrometry investigation of unintentional doping in epitaxial germanium thin films grown on III-V compound by metal-organic chemical vapor deposition

J. Appl. Phys. **111**, 013502 (2012)

Thermodynamic limit to photonic-plasmonic light-trapping in thin films on metals

J. Appl. Phys. **110**, 104501 (2011)

Role of surface vibration modes in Si nanocrystals within light emitting porous Si at the strong confinement regime

J. Appl. Phys. **110**, 023527 (2011)

Photosensitized generation of singlet oxygen in porous silicon studied by simultaneous measurements of luminescence of nanocrystals and oxygen molecules

J. Appl. Phys. **110**, 013707 (2011)

Er³⁺ and Si luminescence of atomic layer deposited Er-doped Al₂O₃ thin films on Si(100)

J. Appl. Phys. **109**, 113107 (2011)

Additional information on *Appl. Phys. Lett.*

Journal Homepage: <http://apl.aip.org/>

Journal Information: http://apl.aip.org/about/about_the_journal

Top downloads: http://apl.aip.org/features/most_downloaded

Information for Authors: <http://apl.aip.org/authors>

ADVERTISEMENT



ACCELERATE AMBER AND NAMD BY 5X.
TRY IT ON A FREE, REMOTELY-HOSTED CLUSTER.

LEARN MORE

Optical properties of heavily boron-doped nanocrystalline diamond films studied by spectroscopic ellipsometry

A. Zimmer,^{1,a)} O. A. Williams,^{2,3} K. Haenen,^{2,3} and H. Terryn¹

¹Research Group Metallurgy, Electrochemistry and Materials Science, Vrije Universiteit Brussel, Brussel 1050, Belgium

²Institute for Materials Research (IMO), Universiteit Hasselt, Diepenbeek 3590, Belgium

³Division IMOMEC, IMEC vzw, Diepenbeek 3590, Belgium

(Received 29 April 2008; accepted 1 September 2008; published online 2 October 2008)

The optical properties of heavily boron-doped nanocrystalline diamond films grown by microwave plasma enhanced chemical vapor deposition on silicon substrates are presented. The diamond films are characterized by spectroscopic ellipsometry within the midinfrared, visible, and near-ultraviolet regions. The ellipsometric spectra are also found to be best described by a four-phase model yielding access to the optical constants, which are found distinct from previous nanocrystalline diamond literature values. The presence of a subgap absorption yielding high extinction coefficient values defined clearly the boron incorporated films in comparison to both undoped and composite films, while refractive index values are relatively comparable. © 2008 American Institute of Physics. [DOI: 10.1063/1.2990679]

At present, nanocrystalline diamond (NCD) films are attracting substantial interest, as such films can be deposited on a plethora of materials.¹ Possible applications include micro/nanoelectromechanical systems (MEMS/NEMS),² biosensors,³ tribology,⁴ optical coatings,⁵ and thermal management.⁶ By adding boron, NCD films can be turned into a *p*-type semiconductor. Conductivity values can be tuned within 11 orders of magnitude, with values ranging between 1×10^{-9} and $100 \Omega^{-1} \text{cm}^{-1}$.⁷ The latter films show a metallic conductivity behavior, even turning superconducting when cooled down to a sufficient low temperature ($\sim 3 \text{ K}$).⁸

Spectroscopic ellipsometry (SE) is a nondestructive optical method that measures the complex ratio R of the Fresnel reflection coefficients of particular directions polarized light (r_p , r_s) and reports the ratio in terms of the ellipsometric angles Ψ and Δ defined by the equation⁹

$$R = r_p/r_s = \tan \Psi e^{i\Delta}. \quad (1)$$

Both *ex* and *in situ* SE for optical characterization of diamond thin films have been used by Collins *et al.*^{10,11} in the beginning of the '90s. SE has also begun to be a powerful technique for microcrystalline diamond films.^{12–15} Concerning NCD films, reports have just appeared over the past few years.^{16–19} Recently Boycheva *et al.*¹⁷ optically characterized NCD/*a*-C composite films prepared by microwave plasma chemical vapor deposition including SE in the range of 250–860 nm. Results were compared with those of polycrystalline films. The use of a Tauc–Lorentz dispersion relation²⁰ in the optical model yields one low value of bandgap ($E_g \sim 1.4 \text{ eV}$). Z.G. Hu *et al.*¹⁹ used also SE to analyze NCD films with a four-phase model in the range of 260–1130 nm. The use of a Sellmeier dispersion relation allows authors to determine the lowest direct bandgap with an approximation (6.9 eV). As for the microcrystalline case, authors propose successive models in order to improve the match between

experimental and fitted data for the nanocrystalline case. This match defines the mean squared error χ^2 , which is a criterion to determine the accuracy of the optical model. However, χ^2 does not verify the physical correctness of the model. The support of other characterization techniques is then necessary to build up a reliable model in order to minimize the range of mathematical solutions in fitting procedure. In this letter, SE has been applied to obtain further information about both optical and morphological properties of B-NCD/Si films. Transmission electron microscopy (TEM) and particularly total reflection measurements have been used to determine the validity of the model.

NCD films of different thicknesses were grown on silicon wafers by a microwave plasma chemical vapor deposition process using an ASTeX 6500 reactor. Before growth, the Si wafers were pretreated using monodisperse nanodiamond aqueous colloid, leading to very high nucleation densities.²¹ The gas flow rate, gas pressure, microwave power, and substrate temperature were 485 SCCM (SCCM denotes cubic centimeter per minute at STP) H_2 , 15 SCCM CH_4 , 35 Torr, 3500 W, and 700°C , respectively. In addition, all films were doped with boron by adding trimethylboron (TMB) to the gas mixture in a $\sim 6500 \text{ ppm}$ $[\text{TMB}]/[\text{H}_2]$ ratio. This concentration leads to a large boron incorporation, leading to metalliclike conduction⁷ and even superconductivity when cooled sufficiently.⁸ To study the influence of the film thickness, the deposition time of film 2-70406 (100 min) was five times higher than that of 2-70313 (20 min).

Coloration rises in the analyzed boron-doped NCD (B-NCD) films: a transition from purple (thinnest film 2-70313) to gray (thickest film 2-70406) is observed. In order to investigate their spectral appearance, experimental colors were measured with a spectrophotometer (Ultrascan XE from Hunterlab). It is based upon an integrated sphere geometry and a D65/10 light source. The measurements were conducted in the 360–750 nm wavelength range. Figure 1 (points) shows the experimental spectra of total reflection for film 2–70313. Corresponding colors can be calculated by means of the 1976 norm of the *Commission Internationale de l'Éclairage* in the $L^*a^*b^*$ -system where the L^* coordinate

^{a)}Present address: Research Group Electrochimie Interfaciale-Corrosion, Institut Carnot de Bourgogne, UMR 5209 CNRS-Université de Bourgogne, Dijon 21078, France. Electronic mail: alex.zimmer@ellipsometrie.fr.

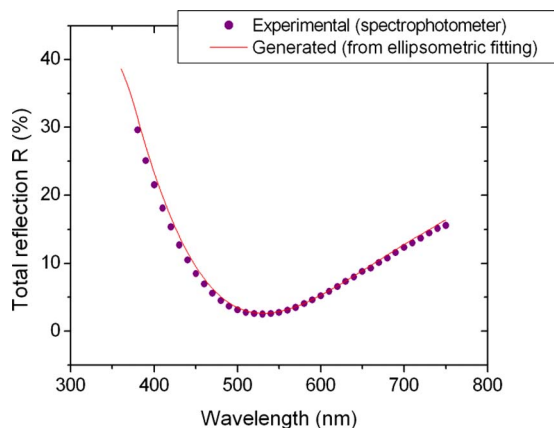


FIG. 1. (Color online) Experimental (points) and generated (line) spectra of total reflection vs wavelength of the B-NCD film (film 2-70313).

gives the variation from white (100%) to black (0%), a^* gives the variation from green (+) to red (−) and b^* the variation from blue (+) to yellow (−). For example, the purple colored film corresponds to $L^*=23.62$, $a^*=23.24$, and $b^*=-20.83$. The ellipsometric measurements were performed in a spectral range of 0.03–4.3 eV at three angles of incidence (60–65–70°) with two ellipsometers from J.A. Woolam Co, Inc. and analyzed with the WVASE32 software. Figure 2 (dashed line) shows the experimental (Ψ, Δ) spectra obtained for the thinnest film. Artifacts near 0.9 eV correspond to overlapping of the two ellipsometers ranges. After an initial step of fitting data with several basic models from the literature (not shown here), two four-phase models gave good overall matches: air/surface rough layer/B-NCD film/Si substrate. For both cases, the dielectric function of the bulk component of B-NCD films was determined by a global fit in

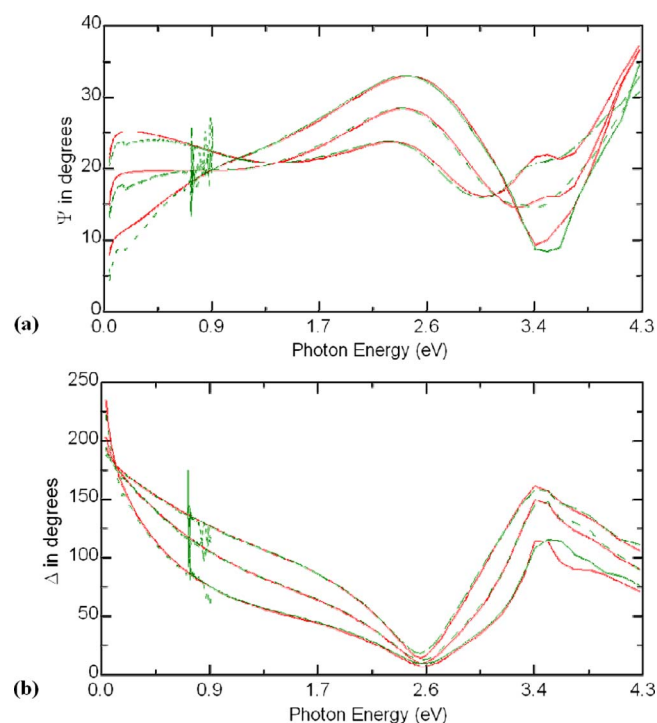


FIG. 2. (Color online) Ellipsometric spectra vs energy of the B-NCD film (film 2-70313). (a) Experimental Ψ (dashed line) and fitted (line) Ψ from model 1. (b) Experimental Δ (dashed line) and fitted (line) Δ from model 1. The three curves correspond to the three employed angles of incidence (65–70–75°).

TABLE I. Summary of best-fit parameters for both models and corresponding selection criteria (χ^2 , mean square error and ΔE^* , color difference).

Model	1	1	2	2
Film	2-70313	2-70406	2-70313	2-70406
Top layer (nm)	32.4	49.5	29.1	42.7
NCD fraction	0.68	0.65	0.73	0.68
Bulk layer (nm)	42.7	333	45.2	426
L.E1 (eV)	0.288	0.146	0.29	0.09
L.A1	150	285	133	713
L.Br1 (eV)	1.76	1.08	1.72	1.07
TL.En/L.E2 (eV)	7.50	8.42	8.70	12.3
TL.A/L.A2	1470	5690	5.3	5.2
TL.C/L.Br2 (eV)	1.24	0.46	0.45	2.9
TL.Eg (eV)	6.67	7.43		
χ^2	2.51	7.52	2.32	3.43
ΔE^*	1.06	8.54	13.8	10.1

the whole spectroscopic range and modeled by combining a Lorentz oscillator (parameters are peak position L.E1, broadening L.Br1 and amplitude L.A1) for the IR part with: (i) a Tauc–Lorentz oscillator [peak position TL.En, broadening TL.C, amplitude TL.A, and bandgap TL.Eg (model 1)] or (ii) a second Lorentz oscillator [L.E2, L.Br2, and L.A2 (model 2)] for the UV-visible part. The dielectric function of the substrate is obtained experimentally by inversion of the ellipsometric angles. The surface rough layer (top layer thickness, NCD/void fraction) is commonly simulated by effective medium theory of Bruggeman.²²

The best fitted curves of film 2-70313 are shown in the Figs. 2(a) and 2(b) (lines) for model 1. Best-fit parameters are illustrated in Table I. Considering only χ^2 values model 2 was found to be more suitable than the first one (lower χ^2 value). Among the energy parameters, the average UV-visible peak position L.E1 of model 2 is about 10.5 eV indicating that the fundamental bandgap E_g is over the experimentally available energy maximum of 4.3 eV. This is also the case in model 1 that gives directly an average value of bandgap of 7 eV. The difference with Boycheva *et al.*¹⁷ on *a*-C/NCD film (1.4 eV) is due to an amorphous carbon feature. Moreover their determination of E_g was done graphically via a Tauc plot and the fitted value of E_g was not shown although it was obtained with a Tauc–Lorentz parameterization. In our case of quasiamorphous carbon free B-NCD films, E_g approaches the lowest direct optical bandgap of single-crystal diamond (7.2 eV) like another estimation done by Hu *et al.*¹⁹ on undoped NCD films. The dispersion relations also indicate a subgap absorption in the midinfrared region, which will be discussed in the next paragraph. For this IR oscillator, both models give close parameters. Among the morphological parameters, the total thickness of the B-NCD films is found to vary between 75 and 383 nm (model 1) or 74 and 469 nm (model 2). A check of the thickness was done by TEM measurements on cross-sections. For the thinnest film, both models agree with TEM value [about 80 nm, Fig. 3(a)] while model 2 overestimates the thickness for the thickest one [about 350 nm by TEM, Fig. 3(b)]. Another check is given by the color difference ΔE^* , which is another description of the difference between the experimental and the generated data (in terms of L^* , a^* , and b^*)

$$\Delta E^* = \sqrt{\Delta L^{*2} + \Delta a^{*2} + \Delta b^{*2}}. \quad (2)$$

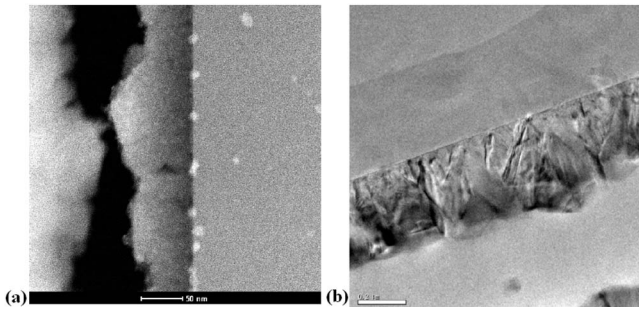


FIG. 3. TEM images: (a) film 2-70313 and (b) film 2-70406.

The lower this value, the better both colors match. If there is a very good agreement between the color generated from the model and the experimentally measured color, it can be concluded that optical model is physically justified. By testing this procedure with both models, model 1 appeared finally the more physically correct (lower ΔE^* values, Table I). Figure 1 (line) also shows the generated reflection spectra obtained from model 1, which matches well the experimental spectra. The color of the surface and the thickness of the film, both confirmed by additional techniques, could also be predicted by ellipsometry (model 1). Concerning surface roughness, the void fractions appear slightly dependent of the bulk thickness (32% and 35%) while top layer thicknesses (32 and 50 nm) confirm the increase in roughness with bulk thickness.¹

Figure 4 gives the refractive index n and extinction coefficient k of the B-NCD films, grown with different deposition times. The refractive index of B-NCD films 2.7–2.2/2.8–2.0 are close to that of recent undoped¹⁹ (~ 2) and composite¹⁶ (2.5–2.4) NCD films but high absorption in the IR is found, yielding unusually high extinction coefficients in the visible-near infrared. This can be explained by the high boron content in the films. It is known that boron induces an acceptor level at 0.37 eV (~ 3450 nm) leading to increased light absorption for higher energies.^{1,23} The fitted peak position of Lorentz oscillator is found near this value.

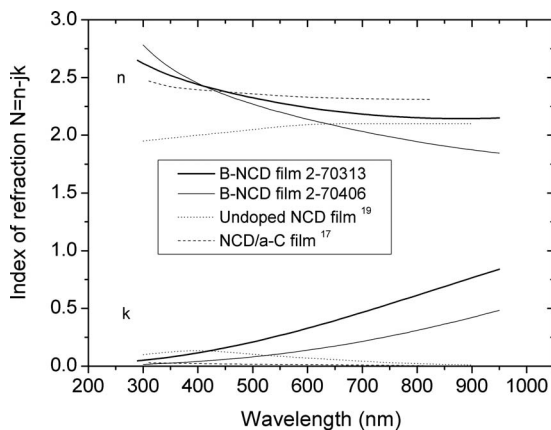


FIG. 4. Complex index of refraction of B-NCD films vs wavelength.

Some variations are also observed between the two samples. Even if the thinnest film gave a reasonable good fit, further improvements could be necessary for the thicker one to clarify the influence of the deposition time on the optical functions of B-NCD films.

In summary, SE experiments have been applied to B-NCD films and a straightforward analysis was obtained with the thinnest sample. Validity of the best-fit parameters has been verified qualitatively with color simulations and TEM. These films possess well-defined optical properties: UV-visible refractive indexes close to that of recent undoped and composite NCD films, unusual nonzero extinction coefficients due to high boron subgap absorption present in IR, and high bandgap approaching the lowest direct electronic transition of single-crystal diamond.

- ¹O. A. Williams and M. Nesládek, *Phys. Status Solidi A* **203**, 3375 (2006).
- ²O. A. Williams, V. Mortet, M. Daenen, and K. Haenen, *Appl. Phys. Lett.* **90**, 063514 (2007).
- ³V. Vermeeren, N. Bijmens, S. Wenmackers, M. Daenen, K. Haenen, O. A. Williams, M. Ameloot, M. van de Ven, P. Wagner, and L. Michiels, *Langmuir* **23**, 13193 (2007).
- ⁴A. V. Sumant, A. R. Krauss, D. M. Gruen, O. Auciello, A. Erdemir, M. Williams, A. F. Artiles, and W. Adams, *Tribol. Trans.* **48**, 24 (2005).
- ⁵P. Achatz, J. A. Garrido, M. Stutzmann, O. A. Williams, and D. M. Gruen, *Appl. Phys. Lett.* **88**, 101908 (2006).
- ⁶J. Philip, P. Hess, T. Feygelson, J. E. Butler, S. Chattopadhyay, K. H. Chen, and L. C. Chen, *J. Appl. Phys.* **93**, 2164 (2003).
- ⁷O. A. Williams, M. Nesládek, M. Daenen, S. Michaelson, A. Hoffman, E. Osawa, K. Haenen, and R. B. Jackman, *Diamond Relat. Mater.* **17**, 1080 (2008).
- ⁸M. Nesládek, D. Tromson, C. Mer, P. Bergonzo, P. Hubik, and J. J. Mares, *Appl. Phys. Lett.* **88**, 232111 (2006).
- ⁹R. M. A. Azzam and N. M. Bashara, *Ellipsometry and Polarized Light* (North-Holland, New York, 1977).
- ¹⁰Y. Cong and R. W. Collins, *Appl. Phys. Lett.* **58**, 819 (1991).
- ¹¹R. W. Collins, Y. Cong, H. V. Nguyen, I. An, K. Vedam, T. Badzian, and R. Messier, *J. Appl. Phys.* **71**, 5287 (1992).
- ¹²N. Cella, H. El Rhaleb, J. P. Roger, D. Fournier, E. Anger, and A. Gicquel, *Diamond Relat. Mater.* **5**, 1424 (1996).
- ¹³T. Pinter, P. Petrik, E. Szilágyi, Sz. Kátai, and P. Deák, *Diamond Relat. Mater.* **6**, 1633 (1997).
- ¹⁴G. Fedosenko, D. Korzec, J. Engemann, D. Lyebdyev, and H. C. Scheer, *Thin Solid Films* **406**, 275 (2002).
- ¹⁵Z. Fang, Y. Xia, L. Wang, W. Zhang, Z. Ma, and M. Zhang, *Carbon* **41**, 967 (2003).
- ¹⁶T. Guzdek, J. Szmids, M. Dudek, and P. Niedzielski, *Diamond Relat. Mater.* **13**, 1059 (2004).
- ¹⁷S. Boycheva, C. Popov, J. Bulir, A. Piegari, and W. Kulisch, *Fullerenes, Nanotubes, Carbon Nanostruct.* **13**, 457 (2005).
- ¹⁸L.-J. Wang, L.-W. Jiang, L. Ren, J.-M. Liu, Q.-F. Su, R. Xu, H.-Y. Peng, W.-M. Shi, and Y.-B. Xia, *Trans. Nonferrous Met. Soc. China* **16**, s289 (2006).
- ¹⁹Z. G. Hu, P. Prunici, P. Hess, and K. H. Chen, *J. Mater. Sci.: Mater. Electron.* **18**, 37 (2007).
- ²⁰G. E. Jellison, Jr. and F. A. Modine, *Appl. Phys. Lett.* **69**, 371 (1996); **69**, 2137.15 (1996) (erratum).
- ²¹O. A. Williams, O. Douhéret, M. Daenen, K. Haenen, E. Osawa, and M. Takahashi, *Chem. Phys. Lett.* **445**, 255 (2007).
- ²²D. A. G. Bruggeman, *Ann. Phys. (Leipzig)* **24**, 636 (1935).
- ²³D. Wu, Y. C. Ma, Z. L. Wang, Q. Luo, C. Z. Gu, N. L. Wang, C. Y. Li, X. Y. Lu, and Z. S. Jin, *Phys. Rev. B* **73**, 012501 (2006).